Journal of New Materials for Electrochemical Systems 13, 147-160 (2010)

Review on Carbon and Silicon Based Materials as Anode Materials for Lithium Ion Batteries

Ali Reza Kamali* and Derek J. Fray

Department of Materials Science and Metallurgy, University of Cambridge, Pembroke Street Cambridge CB2 3QZ, U.K.

Received: June 09, 2010, Accepted: June 28, 2010

Abstract: *Graphite as a traditional anode material in lithium ion batteries cannot fulfil new requirements needing a high energy density. A new generation of high power batteries must be developed using advanced lithium storage materials as electrodes. Disordered and especially nanostructure forms of carbon offer extra sites for both intercalation of lithium and side reactions resulting in a higher reversible and irreversible capacity. Use of these novel forms of carbon depends on the creation of new electrolytes, binders and additives to control side reactions and also development of effective processing technologies. On the other hand, carbon anodes will face strong competition from silicon based materials with their higher capacity. However, the results in the literature highlight important progress in maintaining the capacity of these materials for a small number of cycles, commercial usage of them cannot be imagined without retention of the capacity retention for a much larger number of cycles. This paper reviews the progress toward the production and characterization of new carbon and silicon based materials for using as novel anode materials in lithium ion batteries.*

Keywords: anode, lithium ion battery, carbon, silicon, capacity

1. INTRODUCTION

Rechargeable lithium batteries have been the main source of power for a wide range of modern commercial portable electronic devices [1]. They are also used for the power supply in hybrid electric and electric vehicles [2-5] and can be find wide applications in other industries [6]. On the other hand, regarding to increase in the level and volatility of oil price in recent years and more important, climate change crisis, electric vehicles with good performance and low cost could be a necessity for gasoline-less and zero emission vehicles. Li ion batteries, as the most promising candidate, must meet five categories of goals in order for them to enable the success of electrified vehicles: energy, power, lifetime, safety, and cost [2-5]. Therefore a wide world research has been conduced to develop new generations of these batteries to fulfil the requirements. The great majority of today's lithium-ion batteries typically utilize a lithium metal oxide, Li (Co, Mn or Ni) O_2, as cathode and crystalline graphite as anode with capacities of 160 $mAh.g^{-1}$ (for $LiCoO_2$) and 340 $mAh.g^{-1}$, respectively and $LiPF_6$ as a salt for electrolytes. This electrochemical couple based on intercalation process (Fig.1), provides a cell voltage of approximately 4 V and an energy densities in excess of about 220 $Wh.kg^{-1}$. Although commercially this has proven highly successful cell chemistry, graphite and $LiCoO_2$ both have high coulombic efficiencies

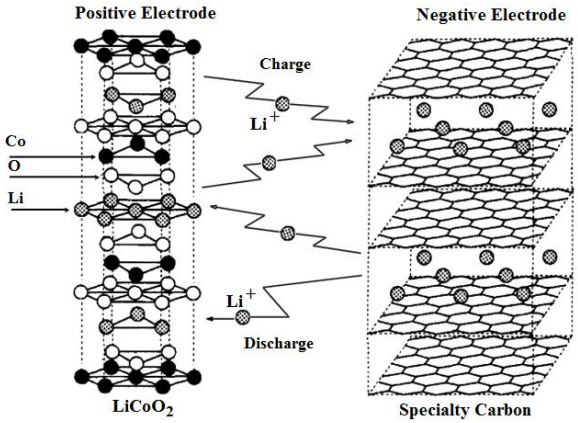

Figure 1. Schematic diagram of the chemical reaction of the lithium ion battery.

*To whom correspondence should be addressed: Email: ark42@cam.ac.uk

Table 1. Characteristics of some emerging anode materials.

Metal	graphite	Li	Si	Ge	Al	Sn
Lithiated compound	LiC_6	Li	$Li_{22}Si_5$	$Li_{22}Ge_5$	AlLi	$Li_{22}Sn_5$
Theorical Capacity($mAh.g^{-1}$)	372	>3800	>3000	1600	993	994
Volume change (%)	9	dendritic grow	323	370	97	300
Reference	[16]	[85]	[87]	[88]	[89]	[90]

more than 95% but rather low capacities [7-9]. Therefore there remains a general requirement for new positive and negative electrode materials to facilitate production of the next generation of these energy storage devices with higher capacity.

According to an assessment, coupling a more advanced anode and cathode with capacities of 600 $mAh.g^{-1}$ and 220 -240 $mAh.g^{-1}$, respectively, could produce a rechargeable cell with energy densities approaching nearly 400 $Wh.Kg^{-1}$[10]. With a similar view, considerable attention has been on development of advanced materials as both anode and cathode applicable in the lithium ion battery, separately. Recent developments in cathode materials has been reviewed in details elsewhere[11,12]. A similar review seems to be necessary on emerging anode materials. These materials can be generally classified as: (a) carbonaceous materials on a lithium intercalation and de-intercalation mechanism (Fig.1), (b) metals and (c) intermetallics both on alloying and de-alloying with lithium mechanism and (d) transition-metal oxides with a mechanism based on a process termed the conversion reaction. This paper reviews the emerging Li ion battery anodes as another development trend of advanced materials, with a focus on silicon and carbon based materials. In this paper, all voltages are stated referenced to that of Li^0/Li^+.

2. CARBON BASED ANODES

The basic block of carbons is a planar sheet of carbon atoms arranged in a honeycomb structure called graphene. Theses carbon sheets are stacked in an order or disordered manner to form crystallites. Carbon materials can be classified into soft carbon (graphitic carbon), hard carbon (disordered carbon) and nanostructured carbon. Lithium ion can be intercalated, more or less, into most kinds of them [13, 14].

2.1. Ordered Carbon

Among different kinds of carbon, natural or artificial graphite has an obvious advantage as a supporting host matrix, that is, when Li is inserted into natural graphite, lithium-intercalated graphitic compounds are reversibly formed at about 0.1–0.2 V [15] offering a theoretical specific capacity of 372 $mAh.g^{-1}$ related to formation of LiC_6. Low volume expansion/contraction of 9% [16] during the lithiation-delithiation is the major benefit of graphite as the anode material. Components of a typical commercial lithium ion cell can be seen in table 1[17].

During the first charge–discharge cycles of the battery, organic solvents including salt anions and impurities will experience reductive decomposition when catholically polarizing the graphite electrode to a sufficiently low potential below 0.8V, thus producing a variety of new chemical substances including C_2H_4, Li_2CO_3, lithium alkyl carbonate and lithium alkoxide. Then, a portion of these new chemical substances will under certain conditions undergo

Table 2. Components of a typical commercial lithium ion cell [17].

Cathode		
material	binder	collector
$LiCoO_2$	PVdF[1]	Al foil
Anode		
material	binder	collector
artificial graphite	SBR[2] +CMC[3]	Cu foil
Electrolyte		
slat	solvent	additive
$LiPF_6$	EC[4]+DEC[5]+EMC[6]	VC[7] + PS[8]

1. Poly vinylidene fluoride 2.styrene butadiene rubber 3.sodium carboxymethyl cellulose 4.ethylene carbonates 5. Diethyl carbonate 6.dimethyl carbonate 7.Vinylene carbonate 8. Propylene sulphite

precipitation from electrolyte solution as a mosaic of solid particles, thus building up layer called the solid electrolyte interphase (SEI) that will eventually cover all the surface of graphite. More detailed studies have revealed that main contribution to the SEI formed on the edge plane of the graphite is the salt anion reduction, whereas the main contribution to the SEI formed on the basal plane of the graphite is the solvent reduction [18, 19]. The SEI layer plays a vitally important role in protecting the graphite electrode from co-intercalation of electrolyte solvents and consequent exfoliation. At the same time, however, formation on this layer leads to an irreversible loss of capacity on the initial charge/discharge cycle of lithium-ion cells. Lu et al. [17] found that both thickness and composition of SEI layer change during the cycling and this is one of the most important reasons that results in the degradation on the cycle performance of the cells. Also, overcharge of the negative carbon electrode leads to the deposition of metallic lithium on it. The deposited lithium rapidly reacts with the solvent to form a surface film on the negative electrode leading to blocking the pores and reducing the magnitude of its working surface area which is another major cause for battery degradation [20]. The ideal SEI layer should be uniform, thin, good lithium ions conductor and insulator for electrons.

There have been two general ways to reduce of irreversible charge or increase reversible charge in graphite anodes: a) modification of additives, binders and electrolyte to obtain an appropriate SEI layer and b) modification of graphite itself. Additives of graphite anode (table 2) are used essentially to obtain an appropriate SEI and improve the cycling. Wang et al. [21] found replacement of commercially used vinylene carbonate and propylene sulphite additives by maleimide (MI)-based compounds as a new additive can reduce the formation of Li_2O and produce thinner SEI to give a

lower resistance route for lithium ion intercalation. Ryou et al.[22] illustrated that the capacity retention of $LiMn_2O_4$/graphite Li-ion cells at a high temperature of 60 ˚C after 130 cycles was significantly improved by about 20% by adding 2 wt.% fluoroethylene carbonate (FEC) additive into the electrolyte of EC/DEC/PC with 1M $LiPF_6$. Also, it was found that the resistance of SEI changes using different salts and solvents as follows: $LiBF_4$ > $LiSO_3CF_3$ > lithium bis (oxalato) borate (LiBOB) > $LiPF_6$ and 1-methyl-2-pyrrolidinone (NMP) > ethyl methyl carbonate (EMC) > methyl butyrate (MB), respectively [23, 24 and references in them]. Also, some polymer gel electrolytes such as ionically cross linked polyampholytic gel electrolyte was evaluated. The results indicated that the formation process of SEI formed in both gel and solution electrolytes are similar [24]. On the other hand, electrode composition can affect the SEI. For example, Sano et al. [25] suggested that a carboxylic group like CMC in graphite binder can act as a catalyst and promotes the SEI formation which prevents the excess electrolyte decomposition on the graphite electrode.

Modification of graphite anode has been another field of research to improve electrochemical performance of the battery. Kulova et al. [26] studied on reducing the irreversible capacity by bringing metallic lithium in direct contact with the graphite electrode in the electrolyte for compensating the lost lithium. By using this method, reversible capacity of graphite increased from a level of 260-290 $mAh.g^{-1}$ to a higher level of 280-300 $mAhg^{-1}$ for first 50 cycles at a current density of 20 $mA.g^{-1}$[26]. It was found that mild air-oxidation of graphite leads to form nanochannels with openings of a few nanometers and up to tens of nanometres. It was suggested that theses nanochannels are formed at the zig-zag and armchair faces between two adjacent crystallites offering a reversible capacity up to 405 $mAh.g^{-1}$[14]. Recently, a reversible capacity of about 370 $mAh.g^{-1}$ after 105 cycles at a rate of 0.2 C has been produced using modified natural flake graphite, where, modification was carried out by mild expanding and carbon coating. This characteristic was attributed to decrease of crystal size of graphite and presence of defects including pores, humps, channels and stacking faults of graphenes [27]. On the other hand it has been found that graphite performance strongly is affected from humidity. It is known that there are active sites including hydrophilic ones in graphite which can absorb water. The absorbed water, in turn, reacts with lithium ion irreversibly to form Li_2O resulting in irreversible capacity. Several attempts have been conducted to increase electrochemical performance by changing the surface structure of graphite and by depositing metals [28-40]. For example, Fu et al.[40] immersed graphite in an aqueous solutions of Cu $(NO_3)_2$ or $AgNO_3$, where, metal ions such as Cu^{2+} and Ag^{+} from the solutions preferentially are adsorbed very active sites at the surface of graphite to form metals and carbides M_xC (M = Cu and Ag). When these sites were effectively removed/covered by deposited metal elements of Cu or Ag, composite electrodes absorbed less water when assembled into model cells in the presence of the high humidity and provided still good electrochemical performance (Fig.2) [40]. Also it has been found that a small amount of metals intercalated in graphite are efficient to enhance the of graphite capacity. For example, a 10% increase in capacity can be obtained by inserting only one atom of tin for 90 carbon atoms [41]. Meanwhile, other characteristics of graphite such as density [42] and particles size [43], to some extent, affect the anode performance.

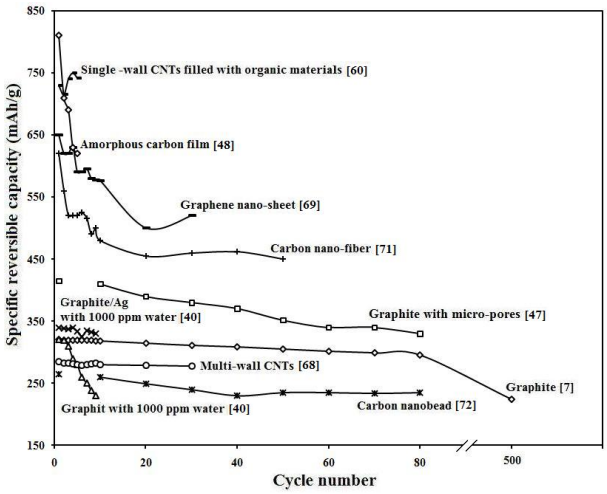

Figure 2. Specific reversible capacity versus cycle number for different kinds of carbonaceous materials.

In spite of these improvements in graphite anode performance, the theoretical and reversible capacities of graphite (Fig.2) are low enough to excite an extensive worldwide research to develop new replacement materials for natural and artificial graphite. In this regard, many researchers have concentrated on use other forms of carbonaceous materials due to intrinsic low capacity of graphite.

2.2. Disordered Carbon

Using disordered carbon instead graphite has been considered to increase lithium capacity, since Dahn et al. [44] proposed that very disordered carbons containing a large fraction of single graphene sheets could have very large capacity of about 740 $mAh.g^{-1}$ if lithium could be adsorbed on both sides of the single-layer sheets. Matsumura et al. [45] proposed that in disordered carbon or carbon with a small crystallite size, Li species are not only intercalated between graphitic layers but also doped at the edge of the graphitic layer and onto the surface of the crystallite. Therefore the capacity of disordered carbon materials can go beyond the theoretical capacity of graphite up to about 450 $mAh.g^{-1}$. Also creation of micro-pores which can offer extra capacity for lithium insertion is an interesting idea. Wang et al. [46] measured a first intercalation-deintercalation capacity of about 430 and 330 $mAh.g^{-1}$, respectively, for hard carbon spherules with microspores. Shim et al. [47] found that a higher capacity than theoretical one can be obtained by forming some micro-pores in natural graphite by using an air heat treatment at 550 °C which leads to 12% weight loss (Fig.2). Subramanian et al. [48] deposited smooth and uniform amorphous carbon on a Cu foil current collector by DC magnetron sputtering technique. The electrochemical performance of the sputtered carbon film was promising with a reversible capacity of 812 $mAh.g^{-1}$ at rate of 0.2 C for the first cycle with an efficiency of 82% due to the low surface area, low film thickness, negligible hydrogen content and low porosity. Recently, other research groups reported reversible capacities less than 410 $mAh.g^{-1}$ using spherical carbon [49], carbon fibers [50], graphitized glass-like carbon [51], carbon-

coated graphite [52] and sulfurized natural graphite by heat-treating or by high energy ball-milling the blend of graphite with sulphur powder [53] and anthracite-based graphite materials [54].

2.3. Carbon Nanostructures

2.3.1. Carbon nanotubes

Carbon nanotubes which are essentially graphene sheets rolled into cylinders have been used as anode materials. Single walled (SWCNTs) [55-60] and multi walled carbon nanotubes (MWCNTs) [61-68] have been proposed as potential substitute for traditional graphite for intercalation. It has been speculated that a high lithium capacity may be obtained in carbon nanotubes if all interstitial sites including inter-shell van der waals spaces, inter-tube channels and inner cores are accessible for lithium intercalation. Purified SWNTs have produced an about 1000 $mAhg^{-1}$ intercalation capacity [55]. To account for the excess lithium capacity, several mechanisms have been proposed including insertion in the open inter-tubular spaces inside the bundles of SWNTs, formation of lithium multi-layers on graphite sheets, formation of Li-C-H bonds, filling micro-cavities and adsorption of lithium on both sides of isolated grapheme layers [55, 56]. However, regarding to a huge nanospace, not only the inner space of the tube, but also the intertubular space in the bundle, SWCNTs bundles may be considered as a major Li storage sites [57]. SWNTs can be reversibly intercalated with lithium up to $Li_{1.7}C_6$ composition, while, their reversible lithium storage capacity can increase to Li_2C_6 after etching. Moreover this saturation composition increases to $Li_{2.7}C_6$ by applying suitable ball milling treatment to the purified SWNTs [58]. It means that SWNTs can contain more than twice the energy density of graphite. Lithium intercalation between graphene layers, defects, microcavities and edge of graphene layers is responsible to such a high capacity [55]. A first lithiation and delithiation capacity of about 1000 $mAhg^{-1}$ and 600 $mAhg^{-1}$, respectively, related to formation of $Li_{2.7}C_6$ has been reported using SWNTs at current density of $50mAg^{-1}$[59]. It should be noted that the electrolyte molecules and the Li ion solvated with the electrolyte molecules can freely enter into the tube interior of the empty SWCNT. Namely, the environment of the inner surface of the SWCNT is similar to the basal plane (the surface a-b plane) of the graphite in the electrolyte which is directly in contact with the electrolyte. It is well known that the basal plane of graphite is not a very good Li ion storage site. It is plausible due to the similar reason why the inner space of the empty SWCNTs does not work for the Li ion storage. It was shown that the encapsulation of organic molecules can increase the stable Li ion storage sites in the tubes [60], So that filling of carbon SWNTs with organic molecule of C_{60} [61] and coronene [60] increased reversible lithium capacity of materials almost 1.7 and 2.5 times more compared to empty one, respectively. SWCNTs filled with organic molecule of coronene produced a first lithiation and delithiation capacity of 1227 $mAh.g^{-1}$ and 736 $mAh.g^{-1}$ at a constant current of 100 $mA.g^{-1}$ (Fig.2) [60].

On the other hand, reversible capacity of MWNTs is reported to be 100-640 $mAhg^{-1}$[62, 63]. A first lithiation and delithiation capacity of 500 $mAhg^{-1}$ and 200 $mAhg^{-1}$ has been obtained using MWNTs pre-doped with lithium [62]. The diffusion coefficients of the Li^+ reaction with MWNTs was found to be in the range between 1×10^{-10} and 4×10^{-10} $cm^2.S^{-1}$ in the range of that of the most carbon materials[64]. Lithium can be inserted between the graphene shells of MWNTs through defect sites within the van der waals gap between two layers of nanotubes [65]. In general, well graphitized MWNTs such as those synthesized by the arc-discharge method have a lower capacity than those prepared by CVD method [55]. An extra capacity of the alkali atoms may be exist also in the cylindrical hollow core of the nanotube, but the mechanism of charge transfer in this case may be quite different from that of the alkali intercalated between each two layer. The metal atoms in the core may not be in direct contact with the wall of the nanotube to permit a fast charge transfer from the alkali atoms to the host and the take part the electrochemical reaction effectively [55]. Insertion of lithium in MWNT has been investigated [66]. It was found that Li insertion is a reversible process and nanotubes do not seem to be affected by the successive lithiation and delithiation [66]. Simulations show that while Li motion through the sidewalls is forbidden, Li ions can enter tubes through topological defects containing at least nine-sided rings or through the ends of open-ended nanotubes. Once inside, their motion is not diffusion limited. These results suggest that damaging nanotube ropes by either chemical or mechanical means will yield better material for electrochemical storage [67]. It has been shown that creation of defects and reduction of tube length to dimensions smaller than 5 microns greatly increases lithium capacity [55]. Yang et al. [68] showed that the first intercalation and de-intercalation capacity of MWNTs with outer diameter of 35–65 nm and length of 150–400 nm is 950 $mAh.g^{-1}$ and 266 $mAh.g^{-1}$(Fig.3), respectively, at the current density of 0.2 $mA.cm^{-2}$ (Fig.2), where, that of MWNTs with outer diameter of 15–30 nm and more than several micrometers in length is less than half. However, unfortunately, in general, not only the large reversible capacities but also the large irreversible capacities have also been reported on carbon nanotubes (Fig.3) which has been attributed to the formation of solid electrolyte interface (SEI) and capillary effects. This layer reduces the actual working of the electrode that is a major limitation due to their high price and capacity degradation (Fig.2). Therefore, reduction of the irreversible capacity is necessary for the practical use of carbon nanotubes as an anode material in Li ion batteries.

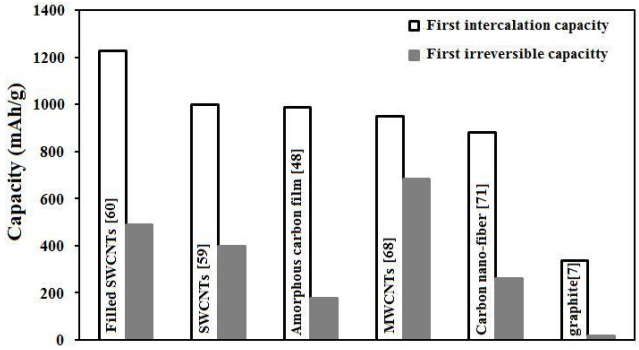

Figure 3. First intercalation capacity and related irreversible capacity for different kinds of carbonaceous materials.

2.3.2. Other forms of carbon nanostructures

A variety of other carbon nanostructures, other than nanotubes, have been evaluated for their probably application as anode materi-

als. Guo et al. [69] produced graphene nanosheets (GNSs) comprising of many disorganized graphenes from artificial graphite by a process comprising of oxidation, rapid expansion and ultrasonic treatment. This disordered structure exhibited an initial intercalation and de-intercalation capacity of about 1250 and 650 mAh.g-1 at a current density of 0.2 mA.cm-2 with a good capacity retention up to 30 cycles (Fig.2), about twice that of the artificial graphite, due to the storage of Li ion on the both sides of graphenes and the presence of functional groups and microspores. Carbon nanofibers have some interesting characteristics such as long length, high surface area and complex porous structure, creating large amount of active sites and reduced charge transport pathways. As a result, they can be considered as anode in the lithium anode battery [70-71]. Carbon nano-fibers comprising of polyacrylonitrile - 30 wt% of polypyrrole presented a reversible capacity of about 450 mAh.g^{-1} after 50 cycles at the current of 50 mA.h^{-1} (Fig.2) and also an initial irreversible capacity of 264 mAh.g^{-1} (Fig.3) due to the formation of SEI layer[71]. These nano-fibers exhibited a relatively convoluted and wrinkled fibrous morphology after 50 cycles, indicating the integrity of CNFs is preserved during charge/discharge cycles [71]. Chang et al. [72] used carbon nanobeads (CNBs) with sizes ranging from 100 to 300 nm to reduce the distance of the intercalation/deintercalation pathway and improve the charge capacity of the lithium ion battery at high current densities. The charge capacity of CNBs was found to be 238 mAhg^{-1}, while that of a high crystalline commercial anode graphite (named MCMB)reaches only 36 mAhg^{-1}, when the charging rate is 1C (372 mA.g^{-1})(Fig.2). Wu et al.[73] observed an improved capacity in carbon nanosprings(CNSs) prepared by a catalytic chemical vapour deposition technology At high current densities comparing to graphite and MWCNTs which could be attributed to the nanometre-sized building blocks as well as the unusual spring-like morphology. This material produced a reversible capacity of about 450 mAh.g^{-1} and 160 mAh.g^{-1} after 100 cycles at a current density of 50 mA.g^{-1} and 3 A.g^{-1}, respectively.

As a conclusion, it can be found from figure 2 that some kinds of carbon nanostructures offer very interesting reversible capacity comparing to others and can be considered as future anode materials. But, before that, some problems such as excessive irreversible charge and technological limits towards industrialization have to be solved, especially regarding the complicated and expensive processes used to their synthesis. In fact it is impossible to imagine a shine industrial future for carbon nanostructures in lake of more effective and cheaper production processes such as a cheap electrolytic process [75-84] which has been developed for production of carbon nanostructures. On the other hand, the majority of ideas to increase capacity in carbonaceous materials has been on basis of preparation of more sites in host material to meet lithium ions, but these sites can be used as development of SEI and therefore increase of irreversible capacity. So, development of new generation of electrolytes, additives or binders seems to be necessary to fulfil characteristic of high reversible and low irreversible capacity in new developed carbonaceous materials.

3. ALTERNATIVE MATERIALS FOR GRAPHITE

Theoretically, using a lithium metal anode is the best way of delivering high energy density due to its very large theoretical capacity of more than 3800 mAh.g^{-1} in comparison to the value of 372 mAh.g^{-1} for LiC_6. However, a pure lithium metal negative electrode is difficult to cycle, has a short cycle life and is extremely dangerous due to the shape change of the electrode upon cycling, dendrite formation and reactions with the electrolyte. Meanwhile, lithium's high reactivity and its low melting point (180 °C) may lead to firing and explosion when for any reason (such as an internal short circuit) the temperature of the cell exceeds 180 °C [10, 85]. There were a few works recently to improve lithium anodes. For example, fullerene has been used to coat the lithium metal anode to improve the electrochemical performance [86] or it was shown that dendrite formation, to some extent, can be inhibited using a special cross-linked gel electrolyte [85]. Among the other possible alternatives for graphite anodes, many studies have been devoted to lithium reactive metals of group IV (Si[87], Ge[88], Al[89], Sn[90]) and group V (Sb[91], Bi[92] ,In[93]) elements. This is due to their ability to react reversibly with large amounts of Li per formula unit to form lithium-metal intermetallics according to following reversible reaction:

$$xLi^+ + Me + xe^- \leftrightarrow Li_xMe \quad (1)$$

where Me is a lithium reactive metal. Silicon has a distinguished position as an emerging alternative material for currently used graphite node material (table 2).

On the other hand, regardless of the element, the formation of Li –metal intermetallics is associated with a large volume change that results in pulverization of the electrode material and a loss electrical contact between the particles upon extended cycling.

There has been a considerable progress in overcoming theses obstacles basically by (a) using a buffer element to absorb the volume expansion of the resultant Li_xMe alloy compounds, (b) carefully choosing the applied voltage window which leads to lack of formation of higher lithium content Li_xMe alloy compounds ,which is in turn associated with a lower volume expansion. The first idea has been appeared in different ways. If we nominate the lithium active metal and lithium inactive metal (or less active metal) as M_A (M'_A) and M_I, respectively, theses ways can be explained as follow:

a) Usage of M_AM_I intermetallic as anode to run reversible charge/discharge reaction of $(M_A)_x(M_I)_y+xLi=xM_ALi+yM_I$ where M_I plays a buffering role.
b) Usage of $(M_A)_{X(}M'_A)_Y$ intermetallic as anode to run the reversible charge/discharge reaction of $(M_A)_x(M'_A)_y +(x+y)Li = xM_ALi+ yM'_ALi$. Formation of lithiated phases occurs in different voltages and therefore one component can act as a buffer for the other one.
c) Reduction of particles size wich leads to the reduction of volume change effect and increase of the apparent diffusivity of lithium ions into the active materials.
d) Production of a composite structure comprising of fine active particles distributed in a preferably amorphous matrix which acts as a buffer.

This paper explores some of the recent development regarding to synthesis and characterization of silicon based materials for application as anode in the lithium ion batteries.

4. SILICON

According to the electrochemical reactions between silicon and lithium, silicon can be alloyed with lithium up to 4.4 atoms of lithium per one silicon atom to form $Li_{22}Si_5$ intermetallic phase or an amorphous phase of equivalent composition Li–18.5 at. % Si. Therefore Si possesses the theoretical capacity of 4200 $mAhg^{-1}$, much higher than those of other anode materials except lithium itself. Silicon which usually forms amorphous phases upon lithiation at room temperature shows severe volumetric changes up to 323% upon cycling leading to create microcracks or pulverization and therefore poor cyclability [87, 94-100]. Other problem associated with Si anodes is their high irreversible capacity at the first cycle due to the phase transformation of the silicon phase alloyed with lithium and the electrochemical reduction of electrolyte solvent on the anode surface[101,102].To overcome the contact losses between silicon, current collector and the electrolyte as a consequence of volumetric changes (i.e. capacity retention) a variety of silicon containing structures have been considered including nanostructured Si-based materials, composites, thin films and nanowires. In general, decreasing the particle size leads to the decrease of macroscopic volume changes of the material to avoid crack formation and consequent degradation. Therefore, production of a nanostructured material would improve the performance of silicon electrode. Although, a nanocrystalline Si can show a high capacity of about 2000 $mAh.g^{-1}$for the first lithiation, the capacity will decrease in following lithiation-delithiation cycles due to aggregation of particles in form of inactive dense blocks, so that the electrode completely fails after 20 cycles [98, 103, 104] showing a simple size reduction of the Si particles cannot effectively eliminate its capacity degradation. Therefore, various composite materials containing different forms of silicon in host matrixes have been investigated in different electrolytes for further improvement [105-112]. C, TiC, SiC, TiN and Cu/C were used as matrixes where the production of these composites included at least one stage of mechanical milling [113-119]. In these composites, the inactive phase would accommodate the mechanical stresses/strains experienced by the active phase and maintain the structural integrity of the composite electrode during the alloying/de-alloying processes. For example, it has been shown when silicon particles are occluded in the lamellar structures of flaked graphite particles, formed a sandwich structure, their volume changes, in a certain extent, are decreased, and improvement of cyclability has been obtained [120]. In addition of graphite, other carbonaceous materials like mesophase carbon, pitch and nanotubes have been used as host matrixes for silicon [121-124]. Zhang et al. [125] added MWCNs to Si-graphite composite by high energy ball milling to utilize the properties of CNTs including high degree of resiliency and conductivity. The working electrode was prepared by casting the slurry of sample powder, carbon black (10%) and polyvinylidene fluoride (PVDF, 20%) dissolved in N-methyl pyrrolidone (NMP) on a copper foil, followed by drying and pressing. The produced anode offered a reversible capacity of 584 $mAh.g^{-1}$ after 20 cycles. Authors proposed when Li reacts with the anode, Li reacts with silicon and natural graphite to form Li_xSi alloy and Li_xC_6, respectively. Also, Li can be inserted into MWNTs between the graphene layers and inner core through the open ends, as well as doped onto the outer surface. The high degree of resiliency and good electric conductivity of MWNTs network mainly contributed to the enhancement of overall reversible capacity and cyclability of the composite anode materials, although the amount of reversible capacity was not so high. Li et al. [126] produced a composite consists of dual phase particles of Si, $FeSi_2$ distributed in the graphite by mechanical ball milling. The composite anode comprised 70 wt. % active materials (Si: $FeSi_2$: graphite = 30:30:40 by wt.), 10 wt. % acetylene black and 20 wt. % PTFE) offered a reversible capacity of more than 600 $mAh.g^{-1}$after 50 cycles over a voltage range of 0.02–1.5 V at a current density of 100 $mA.g^{-1}$. The major problem of this composite was its large irreversible capacity (~650 $mAh.g^{-1}$) due to a large increase in the grain boundaries and active sites of the surface of the composite material, which were produced during mechanical ball milling. Doh et al. [127] produced a composite of Fe–Cu–Si/C by high energy ball milling of elemental raw material and low temperature annealing and observed a reversible capacity of about 385 $Ah.g^{-1}$ after 30 cycles and also a large irreversible capacity of more than 300 $mAh.g^{-1}$ at first cycle upon cycling between 0 and 2 V at 0.253 $mAcm^{-2}$. In another research, a nanosized composite containing Si, Sn , Li_2O , Li_4SiO_4 and graphite was produced by a two step high energy mechanical milling of SnO,SiO and lithium in presence of graphite. The composite electrode revealed a rechargeable capacity of 574 $mAh.g^{-1}$ after 200 cycles at a current density of 0.1 $mAcm^{-2}$. Several factors were considered for the contribution of this improved cyclability. First, the well dispersion of nanosized Sn and Si particles was favourable for the stability of the electrode where the flexible Sn may function as a good electronic conductor. Furthermore, the dispersed graphite and the lithium containing phases formed in the ball milling effectively acted as a buffering matrix and greatly alleviated the volume changes of Si and Sn upon cycling. The potential difference of lithium alloying reaction between Si and Sn could further restrain the volume changes [128]. Wang et al. [129] used SiO_2 and Ni-Si alloys as buffers. In their work, the starting materials of SiO , nickel powder and graphite were ball milled and the ball milled composite underwent to an vacuum heat treatment producing composite powders consisted of Si, Ni, SiO_2, NiO, Ni_2SiO_4 and a series of Si–Ni alloys. The formation of the inactive SiO_2 and Si–Ni alloy phases could accommodate the large volume changes during cycling. The introduction of Ni and graphite could provide better electrical contact during cycling. The composite electrodes revealed a reversible capacity of more than 900 $mAh.g^{-1}$ for nearly 60 cycles upon cycling in a voltage range of 0.02–1.5 V at a current density of $0.1mA.cm^{-2}$, however, irrepressible capacity of about 600 $mAh.g^{-1}$ was also observed in the first cycle. Easily it can be found, although mechanical milling/alloying has been shown to be a powerful technique to produce alloy powders with a homogeneous structure, the high initial irreversible capacity due to large surface area of electrode material is an inevitable limitation. Therefore, great enthusiasm has also been shown to other techniques to produce composites specially by coating the Si particles with secondary materials including carbon/graphite, oxides and nitrides, which may serve either to increase the conductivity of the electrode or to be a buffer that can partially accommodate the volumetric variation without any mechanical milling stage [130-134]. Xie et al. [135] produced crystalline silicon coated mesocarbon microbeads by chemical vapour deposition method followed by treatment at 500ºC. This composite as anode exhibited a low initial coulombic efficiency of 44.7% and

a reversible capacity of about 400 mAh.g^{-1} after 30 cycles upon cycling at a constant current density of 40 mA.g^{-1} between 0.035 and 2.0 V. The low initial charge capacity of 386 mAh.g^{-1} was attributed to less active crystalline Si which undergoes amorphization and becomes activated, which is favourable for long-term cycling. Kim et al. [136] produced Si-coated graphite by plasma enhanced chemical vapour deposition (PECVD) and then a copper silicide coating was created on coated graphite by RF-magnetron sputtering method. They showed that the produced composite offers a reversible capacity of more than 400 mAh.g^{-1} up to 30 cycles. They proposed that the copper silicide seems to act as a buffering layer against the volume change of silicon during the cycling and also provides low interfacial resistance and therefore the smaller impedance affects cycle performance of the electrode. Holzapfel et al. [137] obtained promising results for nanosized silicon/graphite composites prepared by a reductive decomposition of a silicon precursor. The silicon content of this composite (20 wt %) showed a stable capacity of 1000 mAh.g^{-1}, however, the specific capacity has been limited by the small amount of Si in the composite material. Ng et al. [103] reported on carbon-coated Si nanocomposites, containing 44 wt% generally spheroidal nano-crystalline silicon surrounded by an amorphous or semi- amorphous carbon layer produced by a spray-pyrolysis technique. This composite showed a high capacity and coulombic efficiency of 1489 mAh.g^{-1} (Fig.4) and more than 99.5% in the cycling between 0.02-1.20 V at the rate of 100 mA.g^{-1} after 20 cycles [103]. The reversible capacity of a nanocomposite comprising of 44 wt% of Si - 56 wt% disordered carbon was reported to be 1120 mA.g^{-1} after 100 cycles [138].

Kim et al. [139] coated a mixture of Si/Cu by carbon by propylene gas decomposition method and produced a reversible capacity of less than 400 mAh.g^{-1}. Liu et al. [140] Produced carbon-coated Si particles by the CVD process utilizing the pulsed-flow and fluidized bed technique. Carbon coating had a thickness of 500 nm and contained granules of 50 nm diameter. It has been shown that while a Si electrode goes to complete fading at the 8th cycle, the composite offers a capacity of 1000 mAh.g^{-1} until the 57th cycle at a constant current of 300 mA.g^{-1}. They estimated that the C coating and the graphitic component of the conductive additives contribute a capacity of 30 and 179 mAh.g^{-1} in carbon coated electrode and explained that the coating serves to form an exquisite conductive network to allow the fractured Si particles to remain in a good electronic connection with one another. Also, the C coating could serve as a buffer to partially accommodate the volume variation during cycling so that the stability of the entire electrode structure can be improved [40].

Non-carbonaceous materials, also, have been used as matrix in Si-based anode materials. In this regard, cyclability of active Si nanoparticles has been improved, to some extent, using an inactive $CeMg_{12}$ matrix [141]. Zeng et al. synthesized a Si/$LiTi_2O_4$ [142] and Si/TiC [143] nanocomposite films by a sol–gel method in combination with a following heat-treatment process. Through this process, nanosized Si particles were homogeneously distributed in the composite, where, electrochemically less active $LiTi_2O_4$ and TiC could act as the buffering matrix preventing Si from cracking/crumbling during the charging/discharging process offering a reasonable initial and retention capacity (Fig.4). Hwang et al. [144] deposited a composite layer consisting of Mo as inactive component and silicon as active one on Cu foil by an RF-magnetron sputtering system. In this case, molybdenum silicide can be formed due to strong affinity between the Si and Mo which has a very high melting point and excellent mechanical strength so that helps capacity maintenance by forming a buffer of $MoSi_x$ relieving the mechanical stress in the electrode. However, it raises the resistance value of the total cell because the electric resistivity of molybdenum silicide is higher than that of Si and Mo. Those researchers tried to obtain a reasonable balance between two above factors by control of the molybdenum concentration. They obtained an initial capacity of 1319 mAh.g^{-1} that decreased to 1180 mAh.g^{-1} after 100 cycles upon cycling at a constant current of 714 mA.cm^{-2} within a voltage cut-off at 1.0-0.01 V using a composition of $SiMo_{0.79}$. In another study, silicon nitride was used as inactive materials. Zhang et al. [145] reported that 30 wt% Si as active material and silicon nitride as inactive material can offer a charge capacity of 470 mAh.g^{-1}. In another case, lithium silicon nitride and oxynitride composites were prepared by high energy ball milling to explore the influence of precursors on electrochemical properties and capacity of 488 mAh.g^{-1}was obtained [146]. In another work, SiN/bamboo like carbon nanotube composite showed a considerable irreversible capacity in first cycly[147]. Zhao et al. [148] synthesised Si–SnSb dual phase particles according to the following reaction:

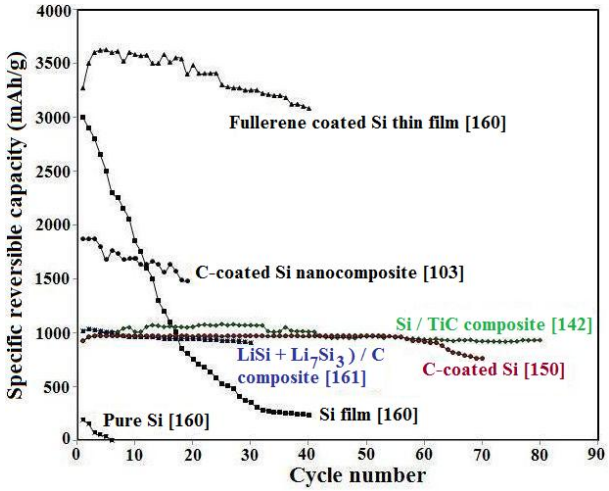

Figure 4. Specific capacity versus cycle number for Si-based anodes

$$2SnO_2 + Sb_2O_3 + 7C + 2Si \rightarrow 2Si\text{-}SnSb + 7CO \quad (2)$$

Then the as-prepared alloy was mixed with pyrolytic polyacrylonitrile (PAN) to synthesize a composite anode. This anode exhibited a reversible capacity of 600 mAh.g^{-1} at current density of 30 mAg^{-1}. Park et al. [149] observed an irreversible capacity of about 1800 and 1000 mAh.g^{-1} at first and fifth cycles, respectively, in encapsulated Si with mesoporous TiO_2 layer.

On the other hand, production of nanowires and their ability as anode materials has been subject of some publications. It has been shown that nanowires can be reasonable candidates for anodes benefiting from one-dimensional diffusion and stress accommodation without cracking or agglomeration [150]. Recently, Cui and

his co-workers [151] have coated amorphous silicon onto carbon nanofibers by chemical vapour deposition (CVD) on a steel substrate using gold nanocatalyst and vacuum growth with silane precursors [152] to form a core-shell structure. The resulted core-shell nanowires showed an initial capacity of about 2000 $mAh.g^{-1}$ which was near the theoretical maximum capacity regarding to silicon content of coated nanowires and also a capacity of more than 1500 $mAh.g^{-1}$ after 55 cycles upon cycling between 0.1-1 V at the rate of C/5. In this case, the carbon core can function as a mechanical support and an efficient electron conducting pathway. Peng et al. [153] and Xu et al. [154] tried to produce silicon nanowires by a less expensive process. They produced crystalline silicon nanowires with a length of approximately 20 μm and a diameter of 100–200 nm by wet etching of boron-doped (100) silicon in aqueous $AgNO_3$/HF. Xu et al**.** [155] prepared a composite anode comprising of this type of silicon nanowires and conventional graphite anode materials by ball milling of silicon / graphite weigh ratio of 15/85. They illustrated that volume expansion during lithation of anode is primarily associated with nanowire diameter swelling without fracture or pulverization. The composite showed an initial lithiation and delithiation capacity of about 811 and 610 $mAh.g^{-1}$,respectively, which was 95% of predicted composite anode lithiation capacity of 853 mA hg^{-1} at current density of 0.1 m.A cm^{-2} in the potential range from 0.01 to 1.5 V . However, only a reversible capacity of 450 $mAh.g^{-1}$ was obtained after 15 cycles.

Some researchers have focused on decrease of active materials thickness to enhance connection between separated active particles and current collector upon cycling offering better cyclability. In this regard, amorphous silicon thin films (50–250 nm) deposited by vacuum deposition methods using organosilane precursors have shown reversible capacities ranging from about 24 to 83% of the theoretical maximum depending on film thickness and preparation methods so that less thickness produced more capacity. Capacity levels for these thin films may be maintained over about 50 several cycles [156].

One other interesting idea has been suggested by some researchers [157-159]: the effect of the volume expansion can be compensated by the production of multilayered Si thin films with metals such as Al, Fe, and Cu nanodots. The theoretical capacity of Al is 2235 $mAh.g^{-1}$ related to the formation of Al_4Li_9 which is much lower than that of Si. But incorporation of Al into Si thin film can decrease the volume change effect due to the smaller volume effect of Al after Li insertion. Also, Al increases the electrical conductivity of electrode leading to improve high rate capability of the electrode. Chen et al. [157] produced an amorphous Si-Al thin film containing 18.69 atom. % of Al by co-deposition from Si target embedded with Al rods on Cu coil. This film delivered a high initial reversible capacity and coulombic efficiency of about 2260 $mAh.g^{-1}$ and 85.9%, respectively, at a rate of 0.05C. One interesting result was that with increase of rate, the Si-Al thin film began to show a capacity even higher than Si thin film. Recently, Arie et al. [160] prepared amorphous polymeric films originated from fullerene on the surface of the silicon thin film by plasma-assisted evaporation methods. The electrochemical performance of these fullerene-coated silicon thin film as an anode material was surprising and demonstrated a high specific capacity of above 3000 $mAh.g^{-1}$ as well as good capacity retention for 40 cycles upon cycling at current density of 0.1 $mA.cm^{-2}$ between 0-2 V (Fig.4), which can be attributed to the fullerene coating layer which enhances the Li-ion kinetic property at the electrode/electrolyte interface. In this case, fullerene films also could act as a buffer layer to reduce the effect of the volume expansion during repeated cycling tests [160].

5. SILICON BASED INTERMETALLICS

Intermetallics, beyond their well-established applications as materials offering interesting mechanical or physical properties, have been considered as candidates for anode materials in lithium ion batteries. In this regard, two families of intermetalics have been received more attentions: (a) Li- Si intermetallics without or with a third element and (b) Me –Si intermetallics where Me is an inactive or less active metal.

5.1. Li-Si (-Me) Intermetallics

Selection of an appropriate Li-Si phase as the active anode material as well as the phase which will be created after lithiation can play an important role in decreasing of the volume expansion/contraction during the cycling. In other words, the volume change could be reduced if the electrochemical cycling is restricted between the Li–Si based intermetallics rather than between pure silicon and an intermetallic. For example, continued reversible alloying and dealloying of Li with $Li_{12}Si_7$ to form $Li_{22}Si_5$ or $Li_{13}Si_4$ is expected to undergo a volume expansion of only about 89% and 54%, respectively, while still retaining a large theoretical specific capacity of about 2571 $mAh.g^{-1}$ and 1470 $mAh.g^{-1}$, respectively [161]. Kanchan et al. [161] produced a Si/C composite by high energy mechanical milling of 42 wt. % Gr–28 wt. % Si–30 wt. % PAN for 12 h followed by a thermal treatment at 1073 K for 6 h. Then a Li–Si/C composite comprising of Li–40 at. % Si alloy dispersed in the C matrix was generated in situ by the controlled electrochemical reaction of Li ions with the mechanically alloyed powders. The final composite comprised of (LiSi + Li_7Si_3) +C which was cycled at a constant current of about 160$mA.g^{-1}$ within the restricted stable potential window of 0.02–1.2 V. The composite had a high specific reversible capacity of about 900 $mAh.g^{-1}$ after 30 cycles (Fig.4). However, restriction of potential window may lead to decrease of the energy density, according to following equation:

$$\text{energy density } (Wh.g^{-1}) = \text{specific capacity } (Ah.g^{-1}) \times \text{potential } (V) \quad (3)$$

Orio et al. [162] has introduced a new intermetellic with composition of $Li_{13}Ag_5Si_6$ and rhombohedral structure. Electrochemical tests showed that this intermetallic is able to insert lithium up to the composition of $Li_{29}Ag_5Si_6$ at a C/20 regime with a reversible specific capacity around 800 $mAh.g^{-1}$ during the first cycling. This compound seems to be an interesting choice for using as anode due to its low density of 3.707 $g.cm^{-3}$, although there is still a need to investigate on the material cyclability. Hang et al. [163] used Li_2SiS_3 as anode material and observed a plateau in the measured voltagrammogram with a large capacity of 2500$mAh.g^{-1}$ appeared in the first reduction process below 0.5 V. Such a large capacity was explained by reduction of Li_2SiS_3 to very small particles of Si and the proceeding formation of Si–Li alloy as follow:

$$Li_2SiS_3 + 4Li^+ + 4e^- \leftrightarrow 2Li_2S + Si \quad (4)$$

$$Si + 4.4Li^+ + 4.4e^- \leftrightarrow Li_4.4Si \quad (5)$$

In the first reduction reaction, the insulating Li_2SiS_3 is converted by semiconducting Si and then by metallic Si–Li alloy enhancing the electronic conduction of the electrode leading to produce high levels of capacity. In spite of the large capacity observed in the first reduction, only a small capacity of about 400 mAh.g^{-1} was observed in the reoxidation process because the electrode becomes insulating upon reoxidation progress, which depresses the electrode reaction and lowers the coulombic efficiency. To overcome this problem, FeS was added as a conductive additive to the Li_2SiS_3. The produced material exhibited a reversible capacity of more than 1200 mAh.g^{-1} after 5 cycles.

5.2. Metal-silicon Intermetallics

NiSi[164,165],FeSi[165],$CrSi_2$[166],$CaSi_2$[167] and Mg_2Si[168-170] have been investigated for possible application as anode materials. Wang et al. [164,165] produced NiSi by high energy ball milling. It exhibited a high lithium storage capacity of 1180 mAh.g^{-1} in the initial lithiation, in which Si acted as the active element to combine with Li to form Li_xSi. But, this reaction was only partially reversible and its capacity degraded upon cycling to reach about 780 mAh.g^{-1} after 25 due to following phase transition sequence:

$$NiSi + xe^- + xLi^+ \rightarrow Li_xSi + Ni \leftrightarrow Ni + Si + xLi^+ + e^- \quad (6)$$

Wang et al. [165] proposed same mechanism for lithium insertion/deinsertion of FeSi-Si offering a capacity of 200 mAh.g^{-1} after 25 cycles.

It was found that the lithiation of Mg_2Si as anode material leads to the formation of Li–Mg and Li–Si binary alloys, directly [169] or through the formation of a ternary phase of Li_2MgSi [170]. Both mechanisms follow the same alloying process leading to a poor cyclability due to high volume expansion. It was demonstrated that a stable reversible capacity of 400 mAh.g^{-1} can be obtained upon the cycling at current density of 50 mA.g^{-1} and a voltage window of 0.02 - 3.0 V by adding 40% carbon to Mg_2Si via ball milling process [171].

6. EFFECT OF MATERIAL CRYSTALLINITY

The most important characteristic of an electrode material is its reversible intercalation capacity which means the amount of electricity that can be reversibly imparted to the electrode during complete lithiation per unite mass of volume. For example LiC_6 and $Li_{4.4}Si$ can be formed during complete lithiation of carbon and silicon materials, which theoretically corresponds to the intercalation capacity of 372 and 4200 mAhg^{-1}, respectively. Another important characteristic of electrode is lithiation-delithiation rate which is controlled by the lithium diffusion rate in the solid phase. Studies have shown a strong dependence of the electrochemical properties on the films crystallinity [172]. However, the crystallinity in anode materials has a dual role and affect on both lithium diffusivity and volume change degradation. Numbers of 10^{-13} cm^2.s^{-1} [173], 10^{-12} cm^2.s^{-1} [174], 2×10^{-11} cm^2.s^{-1} [175] and 10^{-9} cm^2.s^{-1} [175] have been obtained for the lithium diffusion coefficient in amorphous Si thin film , the hydrogenated amorphous silicon thin film, silicon single crystal and nanocrystalline Si film (with a thickness of 1μm and particles size of 10-20 nm), respectively. It can be seen that lithium diffusivity arises by crystallization of amorphous silicon film and by formation of nanocryslline structure. The density of the nanocrystalline film was calculated to be about 1.2 g.cm^{-3}, which is about half of the silicon crystal density. As a result, it may be said that the nanocrystalline film has a loose structure as compared with that of a single crystal, which is allow Li migrate with a faster speed [175]. Although crystalline and especially nanocrystalline silicon offer higher lithium diffusivity, amorphous structures have shown better electrochemical performance upon cycling. It is due to this fact that in crystalline materials, new intermetallics are formed on lithium insertion leading to an inhomogeneous volume expansion in the two-phase regions which can cause cracking and pulverization of the material [176]. It was found that the amorphous Si[177] and amorphous $Si_{0.66}Sn_{0.34}$[178] films remain amorphous throughout all portions of the lithiation and delithiation profile. In another word, there were no two phase regions formed in amorphous samples during the charge - discharge profile offering a homogeneous reversible expansion and contraction without further pulverization. It can be concluded that having an amorphous structure and high conductivity are the key characteristics of an advanced high performance silicon based anode. Furthermore, it has been found that in amorphous films, the capacity loss occurs because contact is lost due to expanding and contracting particles undergoing large volume changes and not because of the pulverization that occurs in crystalline films [179]. According to measured data, the initial charge capacity of amorphous silicon films could be as high as 4000mAh.g^{-1} which can increase to about 4200 mAh.g^{-1} in second cycle for a film with thickness of 50 nm [180], about 2000 mAh.g^{-1} for a thickness of 100nm[156] and about 1600 mAh.g^{-1} for a thickness of 1500 nm[181].

On the other hand, it has been found that crystalline Si converts to the amorphous lithiated silicon phase upon the first reaction with lithium [182,183]:

$$ySi + xyLi \rightarrow (y-x)Si + xa - Li_ySi \quad (7)$$

Crystalline Si and amorphous lithiated Si form a coexistence region of about 3350 mAhg^{-1}[182] leading to a structural mismatch and degradation of the material upon following cycles.

Diffusion coefficient of lithium into nano-crystalline Mg_2Si intermetallic compound (with a thickness of 30- 296 nm) and amorphous Mg_2Si was found to be 5.0×10^{-15} cm^2.s^{-1}and 1.4×10^{-14} cm^2.s^{-1}, respectively [183]. As it can be found, lithium diffusivity in silicon can be 10-10^6 times more than Mg_2Si. Another point is that lithium has a higher diffusivity in amorphous Mg_2Si than that of nano-crystalline Mg_2Si intermetallic compound. Cubic nanocrystalline Mg_2Si film with a thickness of 380 nm exhibited a maximum delithiation capacity of 807 mAh.g^{-1} but lost whole capacity in 50 cycles, while an amourphous one with a thickness of 30 nm exhibited a maximum lithiation capacity of 2241 mAh.g^{-1} and kept majority of the capacity even after 140 cycles [184].

As a short conclusion, it can be said that there was no direct relation between reversible capacity and lithium diffusion coefficient in Si-based materials, because the capacity is affected strongly by volume change of Si upon the cycling. But the situation is different in carbon based materials due to the light effect of volume change. For example, diffusion coefficient of lithium into graphite [174] and porous carbon [185] is 1.2×10^{-10} cm^2.s^{-1} and about 10^{-8} cm^2.s^{-1}

at room temperature. Higher diffusion coefficient of lithium into graphite can be attributed to the large surface area on which lithium diffusion can take place. The higher reversible capacity of graphite with micro-pores [47] than that of commercially used graphite [7] can be found in Fig.2. Carbon powder with a specific surface area of more than 800 $m^2.g^{-1}$ has exhibited a reversible capacity of about 1100 $mAh.g^{-1}$ related to composition of $Li_{2.9}C_6$ [186,187].

7. CONCLUSION

An increasing need to decrease CO_2 emissions has accelerated efforts toward the development of more powerful lithium ion batteries. This fact that capacity of anode has a strong effect on energy density of this kind of batteries has made a global trends and motivation toward the production and characterization of more advanced anode materials than traditionally used graphite because of its low capacity. Lithium content of intercalated compound of carbonaceous materials can be increased from LiC_6 for graphite to higher amounts such as $Li_{2.7}C_6$ for CNTs and $Li_{2.9}C_6$ for carbon nanoparticles offering much more capacity. However, carbon nanostructures and disordered carbon usually offer more suitable sites for both lithium intercalation and side reactions leading to generation of more reversible and also irreversible capacities. While electrochemical performance of carbon nanotubes has been relatively well known, there is not enough knowledge available in the literature on that of carbon nanoparticles. More progress in this field seems to be attainable through following directions :(a) more detailed understanding about parameters affecting electrochemical performance of nanostructure carbonaceous materials and specially carbon nanoparticles. (b) development of new electrolytes and additives which are more compatible with these materials. (c) cost effective production of appropriate nanostructure carbonaceous materials.

On the other hand, silicon as a wonderful lithium storage material can be used as the active component of new high capacity anodes if obstacles can be overcome. First of all, excessive volume change involved during the lithiation - delithiation process has to be appropriately controlled. According to recent investigations reviewed in this paper, this target can be accessed through a set of different new materials including high conductive carbon coated silicon thin film and silicon based composites having amorphous structure. While laboratory-produced materials have presented promising results, commercially usage of silicon based materials as anode material depends on some demonstration of performance and improvement of production techniques. First of all, cyclability of the new materials in more enough cycles has to be demonstrated. On the other hand, the technology level involved in the production of silicon based materials seems to be the critical point towards their commercialization so that development of more easy and cheap production methods is an urgent need.

REFERENCES

[1] J. Yamaki in "Encyclopaedia of Electrochemical Power Sources", 2009, pp.183-191.

[2] Y. Nishi, J. Power Sources, 100, 101 (2001).

[3] T. Kojima, T. Ishizu, T. Horiba, M. Yoshikawa, J. Power Sources, 189, 859 (2009).

[4] M. Anderman, Status and Prospects of Battery Technology for Hybrid Electric Vehicles, Including Plug-in Hybrid Electric Vehicles, Briefing to the U.S. Senate Committee on Energy and Natural Resources, Oregon House, CA: Advanced Automotive Batteries, 2007.

[5] D. L. Anderson in" An evaluation of current and future costs for lithium-ion batteries for use in electrified vehicle power trans", MS Thesis, Environmental Management degree in the Nicholas School of the Environment of Duke University, May 2009.

[6] R. Gitzendanner, F. Puglia, C. Martin, D. Carmenn, E. Jones, S. Eaves, J. Power Sources, 136,416 (2004).

[7] M. Wakihara, O. Yamamoto (Editors) in "Lithium Ion Batteries: fundamentals and Performance", WILEY-VCH, Tokyo, 1998.

[8] K. Ozaea (Editor) in" Lithium Ion Rechargeable Batteries: Materials, Technology and Applications", Wiley-VCH, Strauss GmbH, 2009.

[9] W. A. V. Schalkwijk, B. Scrosati (Editors) in" Advances in Lithium-Ion Batteries", Kluwer Academic/Plenum Publishers, New York, 2002.

[10]R. D. Gupta in "The Electrochemical Production of Tin Filled Carbon Nanotubes and their use as Anode Materials in Lithium-Ion Batteries", PhD Thesis, Department of Materials Science and Metallurgy, December 2008, pp.34-35.

[11]F. F. C. Bazito, R. M. Torresi, Cathodes for Lithium Ion Batteries: The Benefits of Using nanostructured Materials, J. the Brazilian Chemical Society, 17(4), 627 (2006).

[12]J. W. Fergus, J. Power Sources, 195(4), 939 (2010).

[13]G. A. Nazri, G. Pistoia (Editors) in "Lithium Batteries-Science and Technology", Springer, USA, 2009, pp.35.

[14]P. B. Balbuena, Y. Wang (Editorss) in "Ion Batteries-Solid-Electrolyte Interphase", Imperial College Press, Singapore, 2004.

[15]H. Shi, J. Barker, M.Y. Saidi, R. Koksbang, J. Electrochemical Society 143(11), 3466 (1996).

[16]N. Kambe, M. S. Dresselhaus, G. Dresselhaus, S. Basu, A. R. McGhie, J. E. Fischer, Materials Science and Engineering, 40, 1 (1979).

[17]M. Lu, H. Cheng, Y. Yang, Electrochimica Acta, 53, 3539 (2008).

[18]Y. E. Eli, S. F. McDevitt, D. Aurbach, B. Markovsky, J. Electrochemical Society, 144(7), L180 (1997).

[19]J. Yan, J. Zhang, Y.-C. Su, X. G. Zhang, B. J. Xia, Electrochimica Acta, 55, 1785 (2010).

[20]L. S. Kanevskii,and V. S. Dubasova, Russian Journal of Electrochemistry, 41(1), 1 (2005).

[21]F. M. Wang, H. M. Cheng, H. C. Wu, S. Y. Chu, C. S. Cheng, C. R. Yang, Electrochemical Acta, 54, 3344 (2009).

[22]M. H. Ryou, G. B. Han, Y. M. Lee, J. N. Lee, D. J. Lee, Y. O. Yoon, J. K. Park, Electrochemical Acta, 55, 2073 (2010).

[23]S. S. Zhang, K. Xu, T. R. Jow, Electrochimica Acta, 51, 1636 (2006).

[24]W. Chen, Z. Ou, H. Tang, H. Wang, Y. Yang, Electrochimica Acta, 53, 4414 (2008).

[25]A. Sano, M. Kurihara, K. Ogawa, T. Iijima, S. Maruyama, J. Power Sources, 192, 703 (2009).
[26]T. L. Kulova and A. M. Skundin, Russian Journal of Electrochemistry, 38(12), 1319 (2002).
[27]L. Zou, F. Kang, Y. P. Zheng, W. Shen, Electrochimica Acta, 54, 3930 (2009).
[28]K. Endo, H. P. Zhang, L. J. Fu, K. J. Lee, K. Sekine, T. Takamura, Y. U. Jeong, Y. P. Wu, R. Holze, H. Q. Wu, J. Applied Electrochemistry, 36, 1307 (2006).
[29]Y. P. Wu, C. Jaing, C. Wan and R. Holze, Carbon, 41, 437 (2003).
[30]Y. P. Wu, C. Jaing, C. Wan and R. Holze, J. Power Sources, 112, 255 (2002).
[31]M. Dolle, S. Grugeon, B. Beaudoin, L. Dupont and J. M. Tarascon, J. Power Sources, 104, 97 (2001).
[32]M. Li, Y. Tian, Y. Yang, Electrochemica Acta 54, 6792 (2009).
[33]L. Zou, F. Kang, Y. P. Zheng, W. Shen, Electrochemica Acta, 54, 3930 (2009).
[34]S. Komaba, T. Ozeki, K. Okushi, J. Power Sources, 189, 197 (2009).
[35]Y. P. Wu, C. Wan, C. Jiang, S. B. Fang in "Lithium Ion Secondary Batteries", Chemical Industry Press, Beijing, 2002.
[36]S. Kim, Y. Kadoma, H. Ikuta, Y. Uchimoto and M. Wakihara, Electrochemical Solid-State Letters, 4, A109 (2001).
[37]Y. P. Wu, E. Rahm and R. Holze, J. Power Sources, 114, 228 (2003).
[38]Q. Wang, H. Li, L. Q. Chen , X. Huang, Solid State Ionics, 43, 152 (2002).
[39]K. J. Takeuchi, A. C. Marschilok, S. M. Davis, R. A. Leising, E. S. Takeuchi, J. Electrochemical Society, 151, A1188 (2004).
[40]Fu L.J., Zhang H. P., Wu Y. P., Wu H. Q., Holze R., Electrochemical and Solid-State Letters, 8(9), A456 (2005).
[41]J. S. Pena, T. Brousse, D. M. Schleich, Solid State Ionics, 135, 87 (2000).
[42]J. Shim, K. A. Striebel, J. Power Sources, 934, 119 (2003).
[43]Y. S. Park, S. M. Lee, Electrochimica Acta, 54, 3339 (2009).
[44]J. R. Dahn, A. K. Sleigh, H. Shi, J. N. Reimers, Q. Zhong and B. M. Way, Electrochimica Acta, 38(9), 1170 (1993).
[45]Y.Matsumura, S. Wang, J. Mondori, Carbon, 33(10), 1457 (1995).
[46]Q. Wang, H. Li, L. Chen, X. Huang, Solid State Ionics, 43, 152 (2002).
[47]J. Shim, K. A. Striebel, J. Power Sources, 164, 862 (2007).
[48]V. Subramanian, T. Karabacak, C. Masarapu, R. Teki, J. Power Sources, 195, 2044 (2010).
[49]D. Saito, Y. Ito, K. Hanai, T. Kobayashi, N. Imanishi, A. Hirano, Y. Takeda, O. Yamamoto, J. Power Sources, 195(18), 6172 (2010).
[50]S. Yoon, J. H. Ryu, S. M. Oh, C. Lee, J. Power Sources, 194, 486 (2009).
[51]J. M. Skowronski, K. Knofczynski, J. Power Sources, 194, 81 (2009).
[52]H. Nozaki, K. Nagaoka, K. Hoshi, N. Ohta, M. Inagaki, J. Power Sources, 194, 486 (2009).
[53]M. Lu, Y. Tian, Y. Yang, Electrochimica Acta, 54, 6792 (2009).
[54]I. Camean, P. Lavela, J. L. Tirado, A. B. García, On the electrochemical performance of anthracite-based graphite materials as anodes in lithium-ion batteries, Fuel, 89(5), 986 (2010).
[55]Y. Gogodsi (Edithor) in" Nanotubes and Nanofibres",Taylor and Francis,USA,2006, pp.149-150.
[56]S. Yang, J. Huo, H. Song, X. Chen, Electrochimica Acta, 53, 2238 (2008).
[57]Y. Iwai, M. Hirose, R. Kano, S. Kawasaki, Y. Hattori, K. Takahashi, J. Physics and Chemistry of Solids, 69, 1199 (2008).
[58]B. Gao, C. Bower, J. D. Lorentzen, L. Fleming, A. Kleinhammes, X. P. Tang, L. E. McNeil, Y. Wu, O. Zhou, Chem. Phys. Lett., 327, 69 (2000).
[59]B. Gao, A. Kleinhammes, X. P. Tang, C. Bow, L. Fleming, Y. Wu, O. Zhou, Chem. Phys. Lett., 307, 153 (1999).
[60]S. Kawasaki, Y. Iwai, M. Hirose, Carbon, 47, 1081 (2009).
[61]S. Kawasaki, Y. Iwai, M. Hirose, Materials Research Bulletin, 44, 415 (2009).
[62]Z. H. Yang, Y. H. Zhou, S. B. Sang, Y. Feng, H. Q. Wu, Materials Chemistry and Physics, 85, 295 (2005).
[63]G. Maurin, C. Bousquet, F. Henn, P. Bernier, R. Almairac, B. Simon, Solid State Ionics, 136, 1295 (2000).
[64]K. Lin, Y. Xu, G. He, X. Wang, Materials Chemistry and Physics, 99, 190 (2006).
[65]M. S. Dresselhaus, G. Dresselhaus, P. Avouris (Editors) in "Carbon nanotubes, Synthesis, Structure, Properties and applications", Springer, Printed in Germany, 2001, pp.402.
[66]G. Maurin, Ch. Bousquet, F. Henn , P. Bernier, R. Almairac, B. Simon, Chemical Physics Letters, 312, 14 (1999).
[67]V. Meunier, J. Kephart, C. Roland, J. Bernholc, Physical Review Letters, 88(7), 075706-1 (2002).
[68]S. Yang, J. Huo, H. Song, X. Chen, Electrochimica Acta, 53, 2238 (2008).
[69]P. Guo, H.Song, X. Chen, Electrochemistry Communications, 11, 1320 (2009).
[70]L. Ji, X. Zhang, Nanotechnology, 20, 155705 (2009).
[71]L. Ji, Y. Yao, O. Toprakci, Z. Lin, Y. Liang, Q. Shi, A. J. Medford, C. R. Millns, X. Zhang, J. Power Sources, 195, 2050 (2010).
[72]J. C. Chang, Y. F. J. M. Chen, H. T. Chiu, C.Y. Lee, Electrochimica Acta, 54, 7066 (2009).
[73]X. L. Wu, Q. L. Y. G. Guo, W. G. Song, Electrochemistry Communications, 11, 1468 (2009).
[74]Q. Zeng, Z. Li, Y. Zhou, Journal of Natural Gas Chemistry, 15, 235 (2006).
[75]W. K. Hsu, J. P. Hare, M. Terrones, H. W. Kroto, D. R. M. Walton, P. J. F. Harris, Nature, 377, 687 (1995).
[76]W. K. Hsu, M. Terrones, J. P. Hare, H. Terrones, H. W. Kroto, D. R. M. Walton, Chemical Physics Letters, 262, 161 (1996).
[77]W.K. Hsu, J. Li, H. Terrones, M. Terrones, N. Grobert, Y. Q. Zhu, S. Trasobares, J. P. Hare, C. J. Pickett, H. W. Kroto, D. R.

M. Walton, Chemical Physics Letters, 301, 159 (1999).
[78]J. Sychev, N. V. Borisenko, G. Kaptay, K. B. Kushkhov, Russian Journal of electrochemistry, 41, 1079 (2005).
[79]J. Sytchev, G. Kaptay, Electrochimica Acta, 54, 6725 (2009).
[80]G. Z. Chen, X. Fan, A. Luget, M. S. P. Shaffer, D. J. Fray, Journal of Electroanalytical Chemistry, 446, 1 (1998).
[81]A. T. Dimitrov, G. Z. Chen, I. A. Kinloch, D. J. Fray, Electrochimica Acta, 48, 91 (2002).
[82]Q. Xu, C. Schwandt, D. J. Fray, Journal of Electroanalytical Chemistry, 562, 15 (2004).
[83]D. J. Fray, C. Schwandt, A. Dimitrov, US patent No.20080105561,2008.
[84]I. A. Kinloch in "Carbon Nanotubes: Production and concentrated dispersions", PhD Dissertation, Department of Materials Science and Metallurgy, University of Cambridge, Cambridge, 2001.
[85]T. Tatsuma, M. Taguchi, N. Oyama, Electrochemica Acta, 46, 1201 (2001).
[86]A. A. Arie, O. M. Vovk, J. O. Song, B. W. Cho, J. K. Lee, Journal of Electroceram, 23, 248 (2009).
[87]J. C. Arrebola, A. Caballero, J. L. G. Camer, L. Hernen, J. Morales, L. Sanchez, Electrochemistry Communications, 11, 1061 (2009).
[88]C. K. Chen, X. F. Zhang, Nano Letters, 8(1), 307 (2008).
[89]M. J. Lindsay, G. X. Wang, H. K. Liu, J. Power Sources, 84, 119 (2003).
[90]M. Winter, J. O. Besenhard, Electrochimica Acta, 45, 31 (1999).
[91]H. Bryngelsson, J. Eskhult, K. Edstrom, L. Nyholm, Electrochemica Acta, 53, 1062 (2007).
[92]C. M. Park, S. Yoon, S. I. Lee, H. J. Sohn, J. power Sources, 186, 206 (2009).
[93]Y. H. Cui, M. Z. Xue, X. L. Wang, K. Hu, Z. W. Fu, Electrochemistry Communications, 11, 1045 (2009).
[94]C. S. Wang, G. T. Wu, X. B. Zhang, Z. F. Qi, W. Z. Li, Journal of Electrochemical Society, 145, 2751 (1998).
[95]J. H. Ryu, J. W. Kim, Y. E. Sung, S. M. Oh, Electrochemical Solid State Letters, 7, A306 (2004).
[96]B. C. Kim, H. Uono, T. Satou, T. Fuse, T. Ishihara, M. Ue, M. Senna, Journal of Electrochemical Society, 152(3), A523 (2005).
[97]Y. Beaulieu, K. W. Eberman, R. L. Turner, L. J. Krause, J. R. Dahn, Electrochemical Solid-State Letters, 4, A137 (2002).
[98]U. Kasavajjula, C. Wang and A. J. Appleby, J. Power Sources, 163, 1003 (2007).
[99]M. N. Obrovac and L. Christensen, Electrochemical Solid-State Letters, 7, A93 (2004).
[100]X. Yang, Z. Wen, L. Zhang, M. You, Journal of Alloys and Compounds, 4664, 256 (2008).
[101]J. W. Kim, J. H. Ryu, K. T. Lee, S. M. Oh, Journal of Power Sources, 147, 227 (2005).
[102]H. Chen, Z. Dong, Y. Fu, Y. Yang, J. Solid State electrochem, (DOI 10.1007/s10008-009-1001-4) 2010.
[103]S. H. Ng, J. Wang, D. Wexler, K. Konstantinov, Z. P. Guo, H. K, Liu, Angewandte Chemie, 118(41), 7050 (2006).
[104]A. M. Wilson, J. R. Dahn, Journal of Electrochemical Society, 142(2), 326 (1995).
[105]J. Yang, B. F. Wang, K. Wang, Y. Liu, J. Y. Xie, Z. S. Wen, Electrochemical Solid-State Letters, 6, A154 (2003).
[106]N. Dimov, Y. Xia and M. Yoshio, J. Power Sources, 171, 886 (2007).
[107]Z. P. Guo, J. Z. Wang, H. K. Liu, S. X. Dou, J. Power Sources, 146, 448 (2005).
[108]N. Dimov, S. Kugino, M. Yoshio, Electrochimca Acta, 48, 1579 (2003).
[109]V. G. Khomenko, V. Z. Barsukov, J. E. Doninger, I. V. Barsukov, J. of Power Sources, 165, 598 (2007).
[110]X. Yang, Z. Wen, L. Zhang, M. You, Journal of Alloys and Compounds, 464, 265 (2008).
[111]T. Sugimoto, Y. Atsumi, M. Kono, M. Kikuta, E. Ishiko, M. Yamagata, M. Ishikawa, J. Power Sources, 195, 6153 (2010).
[112]Q. Si, K. Hanai, T. Ichikawa, A. Hirano, N. Imanishi, Y. Takeda, O. Yamamoto, J. Power Sources, 195,1720 (2010).
[113]Y. Zhang, Z. W. Fu, Q. Z. Qin, Electrochemistry Communications, 6,484 (2004).
[114]Y. Liu, K. Hanai, J. Yang, N. Imanishi, A. Hirano, Y. Takeda, Electrochemical Solid-State Letters, 7, A369 (2004).
[115]J. H. Kim, H. Kim, H. J. Sohn, Electochemistry Communications, 7, 557 (2005).
[116]P. Patel, II-Seok Kim, P. N. Kumta, Materials Science and Engineering, B116, 347 (2005).
[117]I. S. Kim, G. E. Blomgren, P. N. Kumta, J. of Power Sources, 130, 275 (2004).
[118]I. S. Kim, G. E. Blomgren, P. N. Kumta, Journal of Electrochemical Society, 152(1), A248 (2005).
[119]P. Wang, Y. NuLi, J. Yang, Y. Zheng, International Journal of Electrochemical Science, 1, 122 (2006).
[120]H. Dong, R. X. Feng, X. P. Ai, Y. L. Cao, H. X. Yang, Electrochemica Acta, 49, 5217 (2004).
[121]Z. Lu, L. Zhang, X. Liu, Journal of alloys Compounds, 195, 4304 (2010).
[122]P. Zuo, G. Yin, Z. Yang, Z. Wang, X. Cheng, Materials Chemistry and Physics, 115, 757 (2009).
[123]T. Ishihara, M. Nakasu, M. Yoshio, H. Nishiguchi, Y. Takita, Journal of Power Sources, 146, 161 (2005).
[124]Z. S. Wen, J. Yang, B. F. Wang, K. Wang, Y. Liu, Electrochemistry Communications, 5, 165 (2003).
[125]Y. Zhang, X. G. Zhang, H. L. Zhang, Z. G. Zhao, F. Li, C. Liu, H. M. Cheng, Electrochimica Acta, 51, 4994 (2006).
[126]T. Li, Y. L. Cao, X. P. Ai, H. X. Yang, J. Power Sources, 184, 473 (2008).
[127]C.H. Doh, H. M. Shin, D. H. Kim, Y. D. Jeong, S.-I. Moon, B.-S. J., H.-S. Kim, K. W. Kim, D. H. Oh, A. Veluchamy, Journal of Alloys and Compounds, 461, 321 (2008).
[128]X. Wang, Z. Wen, Y. Liu, X. Wu, Electrochimica Acta, 54, 4662 (2009).

[129]X. Wang, Z. Wen, Y. Liu, X. Xu, J. Lin, Journal of Power Sources, 189, 121 (2009).
[130]M. Yoshio, H. Wang, K. Fukuda, T. Umeno, N. Dimov and Z. Ogumi, Journal of Electrochemical Society, 149(12), A1598 (2002).
[131]N. Dimov, K. Fukuda, T. Umeno, S. Kugino, and M. Yoshio, Journal of Power Sources 114, 88 (2003).
[132]W. R. Liu, J. H. Wang, H. C. Wu, D. T. Shieh, M. H. Yang, and N. L. Wu, Journal of Electrochemical Society, 152, A1719 (2005).
[133]I. S. Kim, G. E. Blomgren, P. N. Kumta, Electrochemical Solid-State Letters, 6, A157 (2003).
[134]M. Q. Li, M. Z. Qu, X. Y. He, Z. L. Yu, J. Power Sources, 188, 546 (2009).
[135]J. Xie, G. S. Cao, X. B. Zhao, Materials Chemistry Physics, 88, 295 (2004).
[136]In-Chul Kim, Dongjin Byun, Joong Kee Lee, J. Electroceram., 17, 661 (2006).
[137]M. Holzapfel, H. Buqa, W. Scheifele, P. Novak, F.-M. Petrat, Chem. Commun., 12, 1566 (2005).
[138]S. H. Ng, J. Z. Wang, K. Konstantinov, D. Wexler, S. Y. Chew, Z. P. Guo, H. K. Liu, J. Power Sources, 174(2), 823 (2007).
[139]H. S. Kim, K. Y. Chung, W. I. Cho, B. W. Cho, Bulletin of the Korean Chemical Society, 30(7), 1607 (2009).
[140]Wei-Ren Liu, Jen-Hao Wang, Hung-Chun Wu, Deng-Tswen Shieh, Mo-Hua Yang, and Nae-Lih Wua, Journal of The Electrochemical Society, 152(9), A1719 (2005).
[141]Z. W. Lu, G. Wang, X. P. Gao, X. J. Liu, J. Q. Wang, J. Power Sources, 189, 832 (2009).
[142]Z. Y. Zeng, J. P. Tu, X. L. Wang, X. B. Zhao, Journal of Electroanalytical Chemistry, 616,7 (2008).
[143]Z. Y. Zeng, J. P. Tu, X. H. Huang, X. L. Wang, J. Y. Xiang, Thin Solid Films, 517, 4767 (2009).
[144]C. M. Hwang, C. H. Lim, J. H. Yang, J. W. Park, J. Power Sources, 194, 1061 (2009).
[145]X. N. Zhang, G. L. Pan, G. R. Li, J. Q. Qu, X. P. Gao, Solid State Ionics, 178, 1107 (2007).
[146]Z. Wen, F. Tian, J. Sun, S. Ji, J. Xie, Rare Metals, 27(2),170 (2008).
[147]S. L. Katar, D. Hernandez, A. B. Labiosa, E. M. Vargas, L. Fonseca, B. Weiner, G. Morell, Electrochimica Acta, 55(7), 2269 (2010).
[148]J. Zhao, L. Wang, X. He, C. Wan, C. Jiang, Electrochimica Acta, 53, 7048 (2008).
[149]S. E. Park, B. E. Kim, S. W. Lee, J. K. Lee, Transactions of Nonferrous Metals Society China, 19, 1023 (2009).
[150]C. K. Chan, P. Hailin, L. Gao, K. McIlwrath, Z. X. Feng, R. A. Huggins, C. Yi, Nature Nanotechnology, 3, 31 (2008).
[151]L. F. Cui, R. Ruffo, C. K. Chan, H. L. Peng, Y. Cui, Nano Letters, 9(9), 3371 (2009).
[152]N. Dimov, S. Kugino, and M. Yoshio, J. Power Sources, 136, 108 (2004).
[153]K. Q. Peng, Y. J. Yan, S. P. Gao, and J. Zhu, Advanced Materials, 14(16), 1164 (2002).
[154]W. Xu, V. Palshin and J. C. Flake, Journal of Electrochemical Society, 156(7), H544 (2009).
[155]Wanli Xu, John C. Flake, Journal of The Electrochemical Society, 157 (1), A41 (2010).
[156]S. Ohara, J. Suzuki, K. Sekine, T. Takamura, J. Power Sources, 136, 303 (2004).
[157]L. B. Chen, J. Y. Xie, H. C. Yu, T. H. Wang, Electrochimica Acta, 53, 8149 (2008).
[158]J. B. Kim, H. Y. Lee, K. S. Lee, S. H. Lim, S. M. Lee, Electrochemistry Communications, 5, 544 (2003).
[159]K. F. Chiu, K. M. Lin, H. C. Lin, C. H. Hsu, C. C. Chen, D. T. Shieh, Journal of Electrochemical Society, 155(9), A623 (2008).
[160]A. A. Arie, W. Chang, J. K. Lee, Journal of Solid State Electrochemistry, 14, 51 (2010).
[161]M. K. Dattaa, P. N. Kumta, J. Power Sources, 194, 1043 (2009).
[162]L. L. Orio, M. Tillard, C. Belin, Solid State Sciences, 10, 5 (2008).
[163]B. T. Hang, T. Ohnishi, M. Osada, X. Xu, K. Takada, T. Sasaki, J. Power Sources, 195, 3323 (2010).
[164]G. X. Wang, L. Sun, D. H. Bradhurst, S. Zhong, S. X. Dou, H. K. Liu, Journal of Alloys and Compounds, 306,249 (2000).
[165]G. X. Wang, L. Sun, D. H. Bradhurst, S. Zhong, S. X. Dou, H. K. Liu, J. Power Sources, 88, 278 (2000).
[166]W. J. Weydanz, M. Wohlfahrt-Mehrens, R. A. Huggins, J. Power Sources, 237, 81 (1999).
[167]J. Wolfenstine, J. Power Sources, 124, 241 (2003).
[168]G. A. Roberts, E. J. Cairns, J. A. Reimer, J. Power Sources, 110, 424 (2002).
[169]H. Kim, J. Choi, H. Sohn, T. Kang, Journal of Electrochemical Society, 146(12), 4401 (1999).
[170]T. Moriga, K. Watanabe, D. Tsuji, S. Massaki, I. Nakabayashi, Journal of Solid State Chemistry, 153, 386 (2000).
[171]J. M. Yan, H. Z. Huang, J. Zhang, Y. Yang, J. Power Sources, 175, 547 (2008).
[172]S. W. Song, K. A. S., R. P. Reade. G. A. Roberts, E. J. Cairns, Journal of The Electrochemical Society, 150(1), A121 (2003).
[173]T. L. Kulova, A. M. Skundin, E. A. Nizhnikovskii, A. V. Fesenko, Russian Journal of Electrochemistry, 42(3), 259 (2006).
[174]T. L. Kulova, A. M. Skundin, Yu. V. Pleskov, E. I. Terukov, O. I. Konkov, Journal of Electroanalytical Chemistry, 600, 217 (2007).
[175]K. Yoshimura, J. Suzuki, K. Sekine, T. Takamura, J. Power Sources, 174, 653 (2007).
[176]T. D. Hatchard, J. R. Dahn, Journal of The Electrochemical Society, 151(6), A838 (2004).
[177]L. Y. Beaulieu, T. D. Hatchard, A. Bonakdarpour, M. D. Fleischauer, J. R. Dahn, Journal of The Electrochemical Society, 150(11), A1457 (2003).

[178]L. Y. Beaulieu, K. C. Hewitt, R. L. Turner, A. Bonakdarpour, A. A. Abdo, L. Christensen, K. W. Eberman, L. J. Krause, Journal of The Electrochemical Society 150(2), A149 (2003).
[179]H. Jung, M. Park, Y. G. Yoon, G. B. Kim, S. K. Joo, J. Power Sources, 115, 346 (2003).
[180]K. L. Lee, Ju. Y. Jung, S. W. Lee, H. S. Moon, J. W. Park, J. Power Sources, 129, 270 (2004).
[181]Kov, E. I. Terukov, I. N. Trapeznikova, Semiconductors, 40(4),468 (2006).
[182]J. Li, J. R. Dahn, J. Electrochem. Soc., 154, A156 (2007).
[183]A. Netz, R. A. Huggins, Solid State Ionics, 175, 215 (2004).
[184]S. W. Song, K. A. Striebel, X. Song, E. J. Cairns, J. Power Sources, 110, 119 (2003).
[185]I. M. Kotina, V. M. Lebedev, A. G. Ilves, G. V. Patsekina, L. M. Tuhkonen, S. K. Gordeev, M. A. Yagovkina, T. Ekstrom, Journal of Non-Crystalline Solids, 815, 299 (2002).
[186]K. L. Van, H. Groult, F. Lantelme, M. Dubois, D. Avignant, A. Tressaud, S. Komaba, N. Kumagai, S. Sigrist, Electrochimica Acta, 54, 4566 (2009).
[187]H. Groult, B. Kaplan, F. Lantelme, S. Komaba, N. Kumagai, H. Yashiro, T. Nakajima, B. Simon, A. Barhoun, Solid State Ionics, 177, 869 (2006).